Optimization of Electrical Oscillators for an Efficient Operation of Resonant Piezoelectric Sensors

Manfred Wich[1], Florian Hubert[2], Jan Helmerich[1], Stefan J. Rupitsch[1]
[1]Department of Microsystems Engineering – IMTEK, University of Freiburg, Germany,
manfred.wich@imtek.uni-freiburg.de
[2]Chair of Sensor Technology, Friedrich-Alexander-Universität Erlangen-Nürnberg, Germany,
florian.hubert@fau.de

***Abstract* -** Many piezoelectric sensor concepts, such as quartz crystal microbalances or piezoelectric temperature sensors, exploit the frequency shift of their resonance frequency as an electric output signal. The resonance frequency of the sensor has to be converted into a frequency-proportional output signal by a subsequent oscillator circuit. Therefore, reliable sensor data processing requires a matching of the resonance frequency and the oscillator frequency at any ambient condition. This contribution focuses on the design of low-cost oscillators with a piezoelectric sensor as the frequency-determining component. Different oscillator topologies will be analyzed regarding their suitability for measurement data processing. In order to achieve a simple and efficient circuit layout, we developed a hybrid design concept based on analytical models and circuit simulations. Experimental results, based on a piezoelectric temperature sensor, prove the proposed design concepts. In the temperature range from -20 °C to 85 °C, an extremely small deviation of less than 0.2 % between the resonance frequency and the oscillator frequency was obtained.

***Keywords* –** Resonant Piezoelectric Sensors, Oscillator Circuits, Meacham oscillator, Pierce oscillator, Heegner oscillator.

I. INTRODUCTION

Resonant piezoelectric sensors are utilized in a wide range of applications [1-2]. For example, ambient temperature can be determined by evaluating the frequency shift of a piezoelectric sensor [3]. Therefore, the resonance frequency f_R must be measured. For this purpose, the piezoelectric sensor is, in most cases, placed in the feedback network of an electrical oscillator as the frequency-determining component (see **Fig. 1(a)**) [4]. Thereby, the oscillator converts f_R to an electric output signal (with an output frequency f_O proportional to f_R). For reliable sensor data processing,

$$f_O = f_R \tag{1}$$

has to be fulfilled.

This contribution provides guidelines for a reliable design of oscillators. Four different oscillator topologies will be analyzed [5] based on the Barkhausen stability criterion [6]. An analysis of the feedback network enables a time-efficient approximation of f_O and a discussion of the influence of the feedback network elements. Additionally, a circuit simulation with LTspice allows for modelling an operational amplifier's characteristics. The circuit simulation, thus, provides a consideration of the loop gain and gives possible value ranges of each circuit element. This hybrid design approach allows us to deduce the suitability of the various oscillator topologies. In addition, we can derive the optimal component values of each oscillator. The proposed design concept was verified experimentally, using a piezoelectric temperature sensor (PI Ceramic PRYY+0111).

II. HYBRID DESIGN CONCEPT

The hybrid design concept can be divided into two separate steps: (i) An analyses of the feedback network and (ii) a subsequent circuit simulation. The analytical model is based on the study of the transfer function of the feedback network $\underline{B}(f)$ (see **Fig. 1(a)**) in terms of the Barkhausen criterion. The circuit simulation is performed by LTspice. For both investigations, the electrical impedance characteristics of the piezoelectric sensor are essential.

The electrical impedance of piezoelectric sensors can be emulated by their Butterworth-van-Dyke equivalent circuit in **Fig. 1(b)** [7]. The values of the equivalent circuit's components (see section III) can be obtained by measuring the electric impedance spectrum with an impedance analyzer (e.g. HP 4194A) and applying a fit formula [8] to the impedance spectrum. The component values of the used piezoelectric temperature sensor result in $L_s = 1.628$ mH, $C_s = 391.4$ pF, $R_s = 23.95$ Ω and $C_p = 876.6$ pF at room temperature, respectively. This leads to a f_R of 199.41 kHz.

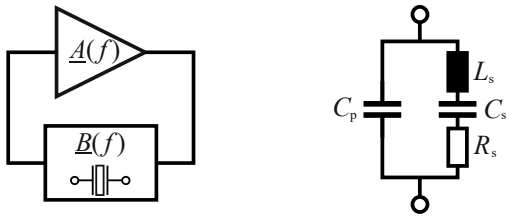

(a) Block diagram of a feedback oscillator. (b) Butterworth-van-Dyke equivalent circuit diagram.

Figure 1: Feedback oscillator (a) with amplifier element $\underline{A}(f)$ and feedback network $\underline{B}(f)$. The feedback network contains a piezoelectric transducer as the frequency-determining component. The Butterworth-van-Dyke (b) equivalent circuit emulates the electrical impedance of the piezoelectric transducer near its resonance frequency.

ISBN 978-3-8007-5835-7

Four different oscillator topologies are investigated and their schematics are shown in **Fig. 2**. The topologies will be optimized in a way that equation (1) is met at any ambient condition. Thus, the piezoelectric sensor will operate at f_R. At this frequency, the piezoelectric sensor behaves almost purely resistively (impedance $\underline{Z}(f_R) = R_s$). An oscillator's peripheral components has to be, therefore, dimensioned in such a way that a stable oscillation occurs at a frequency, at which the piezoelectric sensor behaves purely resistively.

The Pierce oscillator (PO) is one of the most popular oscillator topologies. It consists of an inverting amplifier with two lowpass filters in the feedback network. The basic series resonant oscillator (BO) represents an implementation of an oscillator with minimal component complexity. It consists of only one non-inverting amplifier and a voltage divider in the feedback network. The Meacham oscillator (MO) is a bridge oscillator that resembles the BO in its basic principle, but has another feedback path connected to the inverting input of the amplifier. The two-stage Heegner oscillator (HO) is based on two inverting amplifiers which are fed back by the piezoelectric sensor.

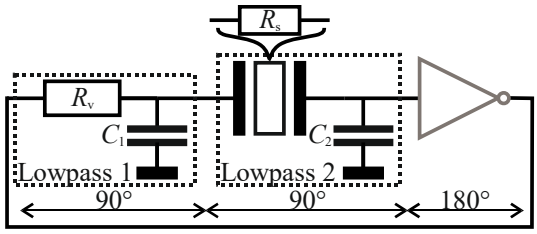

(a) Pierce oscillator.

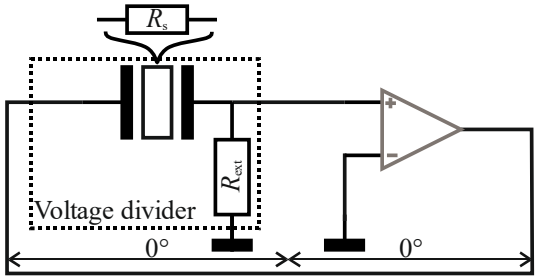

(b) Basic series resonant oscillator.

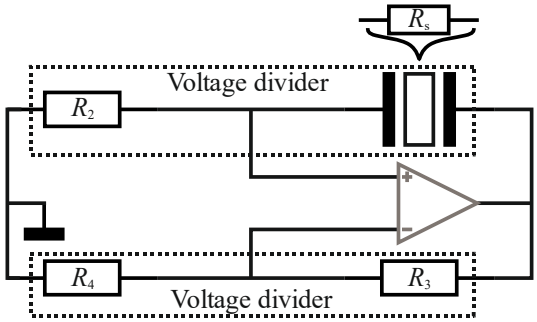

(c) Meacham oscillator.

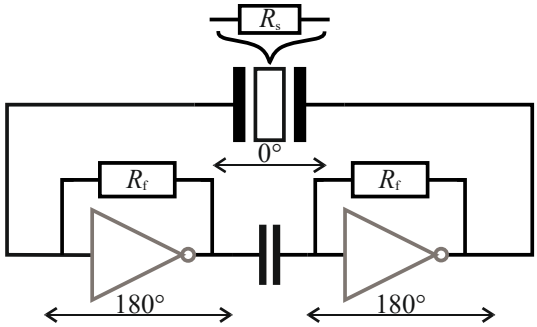

(d) Two-stage Heegner oscillator.

Figure 2: Schematics of the investigated oscillator topologies. The amplifier elements $\underline{A}(f)$ are printed in gray, the feedback networks $\underline{B}(f)$ in black, respectively.

A. Analytical model

The oscillating capability of a feedback oscillator (see **Fig. 1(a)**) can be investigated by using the Barkhausen stability criterion [4, 6]. To apply this criterion, the total loop gain $\underline{T}(f)$, defined by

$$\underline{T}(f) = \underline{A}(f) \cdot \underline{B}(f) \tag{2}$$

must be considered. From equation (2), a phase and an amplitude condition can be derived:

$$\sphericalangle\{\underline{T}(f_O)\} = n \cdot 360°, n \in \mathbb{N}_0, \tag{3}$$

$$|\underline{T}(f_O)| = 1. \tag{4}$$

According to equation (3), f_O is exactly that frequency, at which the phase shift will be zero or a multiple integer of 360°, when the signal passes the entire loop. Equation (4) indicates whether the oscillation is stable at this frequency.

The analytical model is based on the phase condition given in equation (3). Thus, an equation for the total loop gain $\underline{T}(f)$ has to be formulated and analyzed regarding the phase shift. However, the phase shift due to the amplifier $\underline{A}(f)$ is assumed to be ideal (180° for inverting, 0° for non-inverting amplifier(s)). A comparison with the measurement results in section III proves that this simplification is permitted. Therefore, we can reduce the analytical model to the phase shift caused by the transfer function $\underline{B}(f)$.

The analytical model is explained using the PO as an example, since it features the highest complexity. The analyses of the remaining topologies can be found in [5]. The transfer function $\underline{B}(f)$ of the feedback network of the PO's feedback network is calculated to

$$\underline{B}(f) = \left(1 + \frac{R_V}{\frac{1}{j\omega C_1}}\right) \cdot \left(1 + \frac{\left(j\omega L_s + \frac{1}{j\omega C_s} + R_s\right) \Big\| \frac{1}{j\omega C_p}}{\frac{1}{j\omega C_2}}\right) + \left(\frac{R_V}{\frac{1}{j\omega C_2}}\right) \tag{5}$$

by applying Kirchhoff's laws, where j is the imaginary unit.

According to equation (3) and the assumed phase shift of the inverting amplifier, f_O is at that frequency, where the condition

$$\sphericalangle\{\underline{B}(f_O)\} = n \cdot 180°, n \in \mathbb{N}_0 \tag{6}$$

is fulfilled. Thus, equations (5)-(6) enable parameter studies for each individual component of the oscillator's circuitries. In doing so, the effect of the component values on the feed-

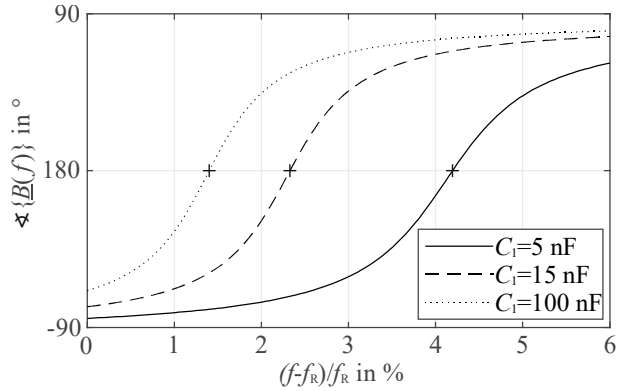

Figure 3: Shift in the phase characteristics of the feedback network by parameter variation of the capacitance C_1 of the PO The cross marks (+) indicate the resulting oscillator frequency f_O (compare equation (6)).

back network's phase characteristics $\sphericalangle\{\underline{B}(f)\}$ and, consequently, f_O can be derived. For instance, increasing the value of C_1 (see **Fig. 3**) reduces the undesired frequency shift between f_O and f_R. Therefore, to meet equation (6), a large value ($C_1 > 100$ nF) must be selected. In this way, the influence of all component values can be examined. **Tab. 1** summarizes the obtained optimal parameters for each oscillator topology. Consequently, the analytical model provides a fast and reliable method to estimate f_O.

Pierce oscillator	Basic series resonant oscillator	Meacham oscillator	Two-stage Heegner oscillator
$R_v\uparrow$ $C_1\uparrow$ $C_2\uparrow$	$R_{ext}\downarrow$	$R_2\downarrow$ $R_3/R_4\downarrow$	$R_f\downarrow$

Table 1: Optimal component values for the investigated oscillator topologies (**Fig. 2**) obtained by the analytical model.

B. Circuit simulation

To determine the limiting values for each circuit component, where a stable oscillation no longer occurs, the amplitude condition of the Barkhausen stability criterion (compare equation (4)) must be considered. Hence, the reduction to its feedback network $\underline{B}(f)$ is not applicable here. A circuit simulation, which enables the inclusion of the amplifier's characteristics, is more significant. Due to optimal component values obtained by the analytical model (**Tab. 1**), the number of parameter variations for each component can be reduced to a minimum and, thus, the time consuming circuit simulation process becomes more efficient.

The oscillation capability of each oscillator topology is examined by a transient simulation with LTspice. From the simulation results, f_O is deduced by applying a Fourier transform. Performing parameter studies, limiting values, where a stable oscillation still occurs, can be determined. For instance, results for the capacity C_1 of the PO are shown in **Fig. 4**. The dashed area indicates the upper limit of C_1. Above this limit, a stable oscillation no longer occurs in the simulation, since the total loop gain is too low. The small deviations between the calculated and simulated frequency f_O stem from a minimal phase shift of the inverting amplifier, which is not included in the analytical model. Thus, the simulation approach completes the analytical model by giving absolute values for the circuit elements.

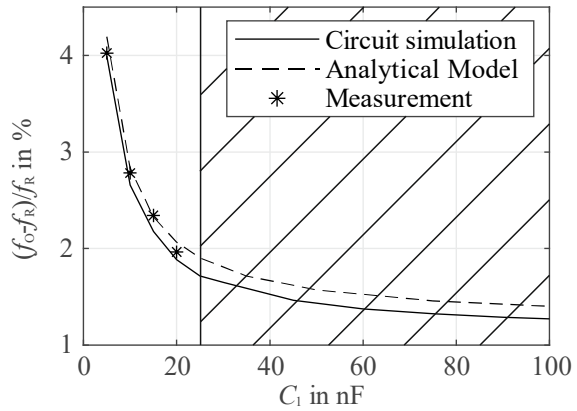

Figure 4: Relative deviation between f_O and f_R under variation of the capacitance C_1 of the PO at room temperature ($T = 25$ °C). In the dashed area, stable oscillation does not occur due to the limited total loop gain.

III. EXPERIMENTAL VERIFICATION

The proposed design concept is verified experimentally. For this reason, the dimensioned oscillator topologies are realized on PCBs. The measured shift in f_O due to, e.g., a variation of C_1 of the PO are depicted in **Fig. 4**. The experimental results clearly proof the proposed hybrid design concept.

Up to this point, the investigations were carried out at room temperature. In the following, we will examine whether the designed oscillators also function at various temperatures and equation (1) is still satisfied at any ambient temperature.

A. Measurement of the temperature-dependent resonance frequency of the piezoelectric sensor

Within its temperature range (-20 °C to 85 °C), the piezoelectric temperature sensor exhibits a shift of f_R between 197.1 kHz and 202.4 kHz (see **Fig. 5**). During this measurement, the piezoelectric sensor was exposed to various temperatures in a climate chamber (ESPEC PL 2KH) and its f_R was determined by an impedance analyzer (HP 4194A). For a reliable temperature measurement, the implemented oscillator should exhibit the same shift of f_O when the piezoelectric sensor is integrated into the designed oscillators.

B. Measurement of the temperature-dependent oscillator output frequency

To determine the temperature-dependent f_O, the realized oscillator is also exposed to various temperatures in a climate chamber. The piezoelectric temperature sensor is integrated into the feedback network of the oscillators. A universal counter (Agilent 53132A) is used to measure f_O. The

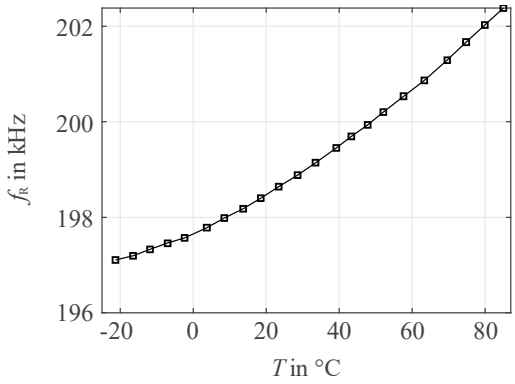

Figure 5: Measured shift in f_R of the piezoelectric sensor as a function of the temperature T. Measurements conducted with impedance analyzer HP4194A.

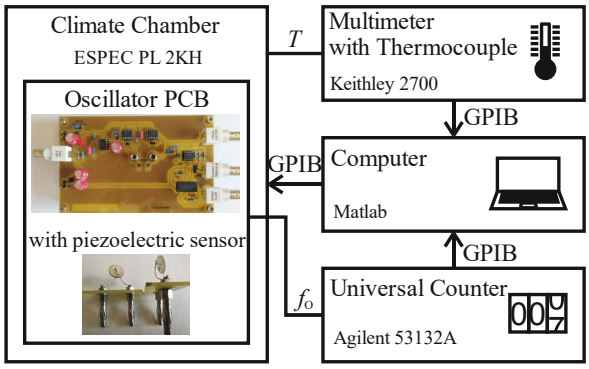

Figure 6: Setup for the measurement of the oscillator frequency in the temperature range from -20 °C to 85 °C.

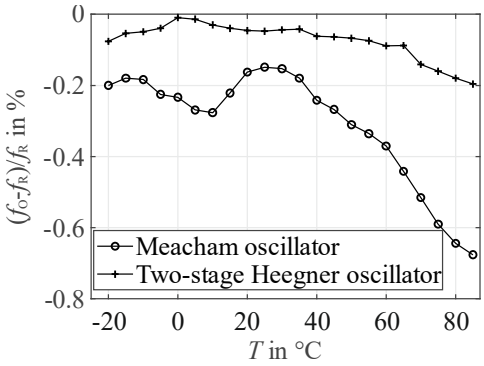

Figure 7: Measurement results showing the extremely small deviation between f_O and f_R.

complete measurement setup can be found in **Fig. 6**. The corresponding measurement results of the two best performing oscillator topologies, the MO and the HO, are shown in **Fig. 7**. The relative deviation between f_O and f_R is found to be extremely small over the entire temperature range from -20 °C to 85 °C. The maximum relative deviation for the HO is extremely low with -0.2 % at 85 °C. Thus, the oscillator, designed according to the hybrid design concept, can convert the temperature-dependent f_R of the piezoelectric sensor into a frequency-equivalent output signal. To put in in another way, the oscillator is capable of oscillating with f_R of the piezoelectric sensor, independently of the ambient temperature.

IV. CONCLUSIONS

A hybrid design concept was presented, which provides a guidance for reliable dimensioning of electrical oscillators. Using this concept, one can investigate the influence of the individual circuit elements on the output frequency of the oscillators. In addition, the limiting values of each component, beyond a stable oscillation no longer occurs, can be determined. The proposed design concept was verified experimentally using a piezoelectric temperature sensor. Within the measured temperature range (-20 °C to 85 °C), a relative deviation of only max. -0.2 % was achieved between the frequency of the oscillator output voltage and the resonance frequency of the piezoelectric sensor. Therefore, the electrical oscillators, dimensioned according to the proposed hybrid design concept, enable a reliable measurement of the resonance frequency of piezoelectric sensors.

V. ACKNOWLEDGEMENTS

The authors would like to thank U. Bollert, Department of Electrical Engineering, Friedrich-Alexander-University Erlangen-Nürnberg, Germany, for preparing the test samples.

VI. REFERENCES

[1] G. Sauerbrey, "*The use of quartz oscillators for weighing thin layers and for microweighing*", Z. Phys., vol. 155, pp. 206–222, 1959

[2] H. Hallil et al., "*Passive Resonant Sensors: Trends and Future Prospects*", *IEEE Sensors Journal,* vol. 21, no. 11, pp. 12618-12632, 2021

[3] J. Ilg et al., "*Impedance-Based Temperature Sensing With Piezoceramic Devices*", *IEEE Sensors Journal,* vol. 13, no. 6, pp. 2442-2449, 2013

[4] R. J. Matthys, "*Crystal Oscillator Circuits*", Malabar, Florida: Krieger Publishing Company, 1992

[5] M. Wich, "*Entwicklung von Oszillatoren für Spannungswandler mit piezoelektrischen EMV-Filtern*", Friedrich-Alexander-Universität Erlangen-Nürnberg, Master Thesis, 2021

[6] M. E. Frerking, "*Crystal Oscillator Design and Temperature Compensation*", New York: Van Nostrand Reinhold Company, 1978

[7] S. J. Rupitsch, "*Piezoelectric Sensors and Actuators: Fundamentals and Applications*", Springer Berlin Heidelberg, 2019

[8] G. Zerong et al., "*Measurement of PT equivalent circuit model parameters based on admittance circle*" 2011 International Conference on Mechatronic Science, Electric Engineering and Computer (MEC), 2011, 20-2